Colloid Polym Sci (2004) 282: 1016–1025
DOI 10.1007/s00396-003-1027-6

ORIGINAL CONTRIBUTION

C. Chauvierre
C. Vauthier
D. Labarre
H. Hommel

Evaluation of the surface properties of dextran-coated poly(isobutylcyanoacrylate) nanoparticles by spin-labelling coupled with electron resonance spectroscopy

Received: 11 September 2003
Accepted: 10 November 2003
Published online: 6 February 2004

C. Chauvierre · C. Vauthier (✉)
D. Labarre
Faculty of Pharmacy,
University of Paris-South XI,
5 rue Jean-Baptiste Clément,
UMR CNRS 8612,
92296 Châtenay-Malabry Cedex, France
E-mail: christine.vauthier@cep.u-psud.fr
Tel.: +33-1-4683-5386
Fax: +33-1-4661-9334

H. Hommel
Laboratoire de Physico-Chimie Structurale et Macromoléculaire, E.S.P.C.I.,
10 rue Vauquelin, UMR CNRS 7615,
75231 Paris Cedex 05, France

Abstract Poly(alkylcyanoacrylate) nanoparticles are developed as carrier for the in vivo delivery of drugs. In this area of research, one of the major challenges is to design nanoparticles able to carry a drug to a specific site in the body. This appears to be mainly governed by the surface properties of the carrier. Results from previous independent studies suggest that the way dextran chains are arranged at the nanoparticle surface can affect the in vivo fate of the carrier. Thus, the purpose of the present study was to investigate for the first time whether electronic paramagnetic resonance (EPR) could highlight a difference between the physico-chemical surface properties of dextran-coated nanoparticles obtained by two different emulsion polymerisation mechanisms of isobutylcyanoacrylate. Poly(isobutylcyanoacrylate) nanoparticles were prepared either by anionic or by radical polymerisation, initiated in both cases by dextran. The respective copolymers self-organised as nanoparticles. Dextran chains located at the nanoparticle surface could be labelled with a free nitroxide radical containing a probe and EPR analysis could be performed on freeze-dried nanoparticles, rehydrated nanoparticles and dispersed nanoparticles in water. The mobility of dextran chains appeared to differ according to the degree of hydration of the systems. More interestingly, EPR spectra clearly highlighted differences in dextran chain mobility comparing the nanoparticles obtained by radical and anionic polymerisation. Therefore, this technique opens an interesting prospect of investigating surface properties of polysaccharide-coated nanoparticles by a new physico-chemical approach to further correlate the mobility of the polysaccharide chains with the fate of the nanoparticles in biological systems.

Keywords Electronic paramagnetic resonance · Nanoparticles · Poly(isobutylcyanoacrylate)-dextran copolymers

Introduction

An exciting application of colloidal particles based on biodegradable polymers is their development as carriers for the in vivo delivery of drugs [1, 2, 3]. Currently, the most promising biodegradable particles consisting of poly(alkylcyanoacrylate) (PACA) nanoparticles are in clinical development for cancer therapy [4, 5, 6, 7, 8, 9, 10, 11, 12].

Synthesis of PACA nanoparticles is usually achieved by emulsion polymerisation of alkylcyanoacrylate, initiated by hydroxyl groups of dextran and resulting in an anionic polymerisation. The nanoparticles have given very interesting results in achieving drug delivery by

local or oral routes of administration [13, 14, 15, 16]. After intravenous injection, these nanoparticles are rapidly removed from the bloodstream due to a massive uptake by macrophages of the mononuclear phagocytes system (MPS). Thus, they mainly concentrate in the liver and spleen where interesting therapeutic applications could be proposed [17, 18, 19, 20]. This specific distribution of the nanoparticles could be related to their recognition as foreign bodies by macrophages. This follows a complex mechanism called opsonisation and involves blood proteins adsorption and activation of the complement system due to interactions of proteins with the nanoparticle surface.

Presently, the major challenge is to design nanoparticles able to carry a drug to a specific site in the body by escaping macrophage capture and enabling specific recognition of a biological target at a molecular level. To this end, new polymeric nanoparticles endowed with modified surface properties have been proposed. To reduce opsonisation, the most popular approach has been to create a steric barrier made of poly(ethylene oxide) (PEO) on the nanoparticle surface to repel blood proteins [21, 22, 23, 24, 25]. A reduction in opsonisation and/or uptake by the MPS was obtained with the PEO-coated nanoparticles when compared with the uncoated nanoparticles [26, 27, 28, 29].

Other hydrophilic polymers, including dextran, were shown to produce a steric repulsive effect. For instance, dextran-coated polystyrene plates showed different capacities to prevent fibrinogen adsorption whether the polysaccharide was grafted in the side-on or the end-on position, resulting in a difference in the conformation of the dextran chains on the polymer surface [30]. From this report, it appears that the way dextran chains are attached to the polymer surface is affecting protein adsorption. Concerning complement activation, soluble dextran is a poor complement activator whereas crosslinked dextran particles such as Sephadex beads are well known as powerful activators [31]. Dextran-coated nanoparticles were also shown to produce different complement activation depending on the emulsion polymerisation mechanism responsible for their formation. End-on-bound dextran-coated poly(methyl methacrylate) nanoparticles obtained by radical polymerisation were low complement activators like soluble dextran, and could circulate in the bloodstream for hours after intravenous injection into mice [32]. In contrast, dextran-coated PACA nanoparticles obtained by anionic polymerisation of alkylcyanoacrylate induced strong complement activation and were rapidly taken up by the MPS organs after intravenous injection into mice [33, 34, 35].

Taking into account the different polymerisation mechanisms used to prepare both kinds of dextran-coated nanoparticles, it can be expected that the conformation of dextran chains at the nanoparticle surface is different, leading to the observation of different in vivo fates, but a major obstacle to investigating this hypothesis is finding a suitable and relevant method which could highlight possible differences in the conformation of dextran chains on the surface of spherical particles with a diameter of a few hundreds of nanometers. Another restriction on such a study is that the method should be used on hydrated nanoparticles because, when interacting in vivo with proteins, the nanoparticles are surrounded by an aqueous environment. The purpose of the present study was therefore to investigate the application of a technique based on electron paramagnetic resonance (EPR) of free radicals. This method is able to discriminate between highly mobile (liquid-like) and slowly mobile (solid-like) spin labels on the basis of their magnetic relaxation times. Thus, such a label was covalently coupled to the dextran chains surrounding PACA nanoparticles obtained either by anionic or radical polymerisation [36, 37, 38]. EPR spectra of the coupled label were then recorded to investigate its mobility, which should be related to the mobility of the dextran hydrophilic chains carrying the label and attached to the nanoparticle surface [39].

Materials and methods

Materials

Isobutylcyanoacrylate (IBCA) was kindly provided by Loctite (Dublin, Ireland). Dextran (MW 15–20,000 g/mol), cerium (IV) ammonium nitrate, nitric acid and trisodium citrate dihydrate were purchased from Fluka (Saint-Quentin Fallavier, France). Carbodiimidazole and 4-amino-2,2′,6,6′-tetramethyl-piperidine-*N*-oxyl (4-amino-TEMPO) were supplied respectively by Sigma and Aldrich (Saint-Quentin Fallavier, France). All chemicals were reagent grade and used as purchased.

Preparation of dextran-coated poly(isobutylcyanoacrylate) (PIBCA) nanoparticles

Radical polymerisation Dextran (0.1375 g, i.e. around 0.85 mmol glucose units or 8×10^{-3} mmol dextran chains) was dissolved in 8 ml of 0.2 M nitric acid in a glass tube at 40 °C, under gentle stirring and argon bubbling. After 10 min, 2 ml of a solution of 8×10^{-2} M cerium (IV) ammonium nitrate in 0.2 M nitric acid, and 0.5 ml of IBCA were successively added under vigorous stirring. Argon bubbling was maintained for 10 min and stopped. The reaction was allowed to continue at 40 °C under gentle stirring for 40 min. After cooling to room temperature, NaOH was added to raise the pH to a value ranging from 7.0 to 7.5 after addition of 1.25 ml of 1.02 M trisodium citrate, in order to protect the polysaccharide against acidic hydrolysis.

Anionic polymerisation Dextran (0.1375 g) was dissolved in 10 ml of 0.2 M nitric acid in a glass tube at 40 °C, under gentle stirring and argon bubbling. After 10 min, 0.5 ml of IBCA were added under vigorous magnetic stirring. Argon bubbling was maintained for additional 10 min and stopped. The reaction was allowed to continue at 40 °C under gentle stirring for 40 min. After cooling to room temperature, NaOH was added as described above.

Spin-labelling of particles by 4-amino-TEMPO

The particle suspensions were filtered through a 1.2 μm membrane filter (Sartorius, Göttingen, Germany) to remove possible aggregates. The filtered suspensions (3 ml) were dialysed twice for 2 h against 1 l of osmosed water and once against 0.01 M phosphate buffer, pH 7.4 (Sigma, Saint Louis, Mo., USA), by using a Spectra/Por dialysis membrane (MWCO 100,000 Da, Spectrum, Houston, USA). The purified suspensions were then allowed to react with 27 mg (0.166 mmol) carbonyldiimidazole (CDI) and 11 mg (0.064 mmol) 4-amino-TEMPO dissolved in 0.5 ml of phosphate buffer, for 48 h under magnetic stirring at room temperature. The labelled particles were purified by dialysing three times the suspensions against 1 l of phosphate buffer for 2 h and using the same dialysis membrane as described above. In this method of labelling, CDI reacts with the hydroxyl groups of dextran allowing a specific linkage of the label to the dextran chains [40]. A typical chemical formula of the labelled dextran is given in Fig. 1.

Particle size analysis

The mean diameter and the size distribution of the particles were determined at 20 °C by quasi-elastic light-scattering using a Nanosizer N4 PLUS (Beckman-Coulter, Villepinte, France). The scattered light was measured at 90°. Each sample of particles was analysed at three different steps of the synthesis: just after polymerisation, after filtration and dialysis, and after labelling and final purification. The samples were diluted in MilliQ water to give a signal level ranging from 5×10^4–1×10^6 counts s^{-1} as recommended by the manufacturer of the light-scattering apparatus. The apparatus provides the mean hydrodynamic diameter, the standard deviation of the size distribution and the polydispersity index. Each determination was performed in triplicate.

Freeze-drying

The labelled particles were frozen at −18 °C and freeze-dried for 48 h in a Christ alpha 1–4 freeze dryer (Bioblock, Illkirch, France) without cryo-protecting agent.

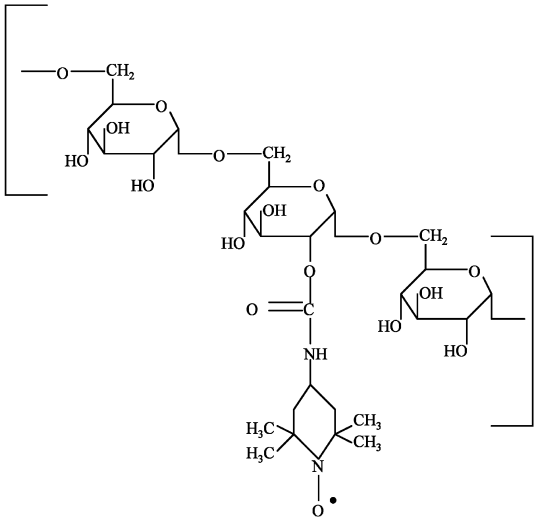

Fig. 1 Typical chemical formula of spin-labelled dextran

EPR spectroscopy

Apparatus and samples EPR spectra were obtained by using a Varian E-4 spectrometer (Varian, Paolo Alto, Calif., USA) operating in the X-band at 9.15 GHz. The spectrometer cavity worked in the TEM_{102} mode. The oscillating magnetic field was maximal at the centre of the cavity, whereas the electric field was minimal. Flat cells were used as sample holder because of the high dielectric constant of the solvent used for the particle dispersions, which induces high-energy loss. The labelled samples consisted of either never-freeze-dried particles dispersed in a large amount of water (dispersed particles), freeze-dried particles (freeze-dried particles), or freeze-dried particles rehydrated with a few drops of water (rehydrated particles).

Analysis of spectra The shape of EPR spectra of nitroxide free radicals is very sensitive to the Brownian motion of the label. The absorption results from transitions between the energy levels of the spin Hamiltonian, H [41]:

$$H = SgB + IAS$$

where $S = 1/2$ is the spin of the unpaired electron, $I = 1$ the spin of the nitrogen nucleus, g the electronic Zeeman splitting tensor, A the hyperfine tensor, and B the magnetic field. The gyromagnetic tensor g and the hyperfine tensor A, which appear in the spin Hamiltonian, have been evaluated using as reference the spectra of the label at room temperature and at the temperature of liquid nitrogen in X-band and Q-band spectroscopy. The best fit was found for $g_{xx} = 2.0088$, $g_{yy} = 2.0058$, $g_{zz} = 2.0022$, $A_{xx} = 5.3$, $A_{yy} = 4.6$, and $A_{zz} = 33.55$. For polar solvents such as water these values are somewhat shifted, but the reference spectrum at nitrogen temperature is difficult to record without breaking the tube, and no attempt has been made to include this correction here. When the motion is relatively fast, i.e. typically with rotational correlation times between 3×10^{-9} s and 3×10^{-11} s, the motion averages the anisotropic interactions and the spectrum consists of three well-resolved Lorentzian peaks. This can be simulated by using a computer according to the theory of Kivelson [42]. If the motion is relatively slow, i.e. typically with rotational correlation times above 10^{-8} s, the anisotropic part of the Hamiltonian spin is not averaged and broader peaks, shifted compared to the previous ones, are produced. They are explained by the much more comprehensive Freed theory [41]. Very often, for polymers at interfaces the experimental spectra appear as a superposition of the two kinds previously distinguished. The method of analysis of the spectra is explained in Fig. 2 [39]. The experimental spectrum is the first derivative of the absorption whereas the population is its first integral. To ensure a valid integration it was checked each time that the "absorption" spectra returned exactly to zero at the end of the integration domain. It follows then, that the integral must approach a constant value. A narrow line with a high intensity can result in a small population, whereas a broad line even with a low intensity can result in a very high population. As the comparison between fast and slow population is made each time inside the same spectrum, the overall intensity is not relevant for this result. The derivatives are simulated and the precision could be around 10%, but for the integrals the precision should be even better. The physical interpretation of this shape of the spectra is to assign narrow lines to loops and tails protruding in solution with a fast motion, whereas the broad lines pertain to trains adsorbed on the particle surface and experiencing a hindered motion. It is therefore the essential heterogeneous character of the system which is reflected in the spectra.

Results and discussion

Milky suspensions showing a Tyndall effect have been obtained through the radical and anionic polymerisation

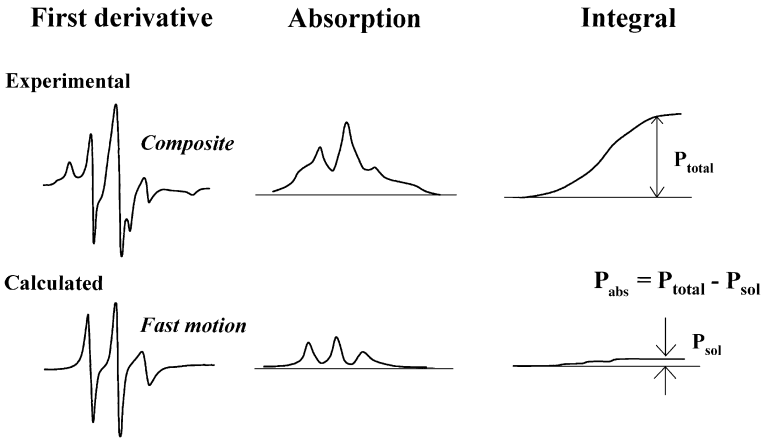

Fig. 2 Method of analysis of the spectra. The *experimental* spectrum is the *first derivative* of the absorption whereas the population is its first *integral*. A narrow line even with a high intensity can result in a small population, whereas a broad line even with a low intensity can result in a very high population. As the comparison between fast and slow population is made each time inside the same spectrum, the overall intensity is not relevant for this result

processes. No polymer aggregates were formed during the course of the radical polymerisation, whereas a few aggregates appeared during the course of the anionic polymerisation. The sizes of the polymer particles obtained at the different steps of the preparation [i.e. after synthesis (step 1), after filtration and dialysis (step 2), and after labelling and final purification (step 3)] are reported in Table 1. The mean hydrodynamic diameter of the particles resulting from radical polymerisation was 162 ± 47 nm with a polydispersity index of 0.127. The characteristics of the particles were not substantially modified during the purification and labelling steps. The mean hydrodynamic diameter of the particles resulting from anionic polymerisation was 337 ± 138 nm with a polydispersity index of 0.514. The size, standard deviation and polydispersity index decreased after filtration and dialysis. After labelling and further purification, the size and polydispersity index of these particles increased three times, and the standard deviation five times.

The EPR spectra obtained with the labelled particles, either freeze-dried, rehydrated or dispersed, are shown in Fig. 3, Fig. 4 and Fig. 5 respectively. The intensity of the signals provided by the label was high enough to analyse the spectra. It indicated that the label was grafted on the nanoparticle surface in such a way that the label molecules were diluted and that there were no dipolar interactions between spins.

Broad and typical signals for powders were obtained with freeze-dried particles (Fig. 3). The spectra could not be analysed according to the theory of Kivelson [42], since the movements of the label were too slow.

Composite spectra highlighting three narrow Lorentzian peaks were given by the analysis of the rehydrated particles (Fig. 4) and of the dispersed particles (Fig. 5). The shape and intensity of the signals obtained at a similar level of amplification were obviously different and depended on the types of particles for the dispersed samples. Indeed, the Lorentzian peaks presented

Table 1 Size of the particles obtained by either a radical or an anionic polymerisation mechanism and modified by the spin-labelling process. The mean hydrodynamic diameter, standard deviation (*SD*) of the size distribution and polydispersity index (*PDI*) (dimensionless) were determined at three steps: just after polymerisation (*1st step*), after filtration and dialysis (*2nd step*), and after labelling and final purification (*3rd step*). The results are the average of three determinations on the same sample

Type of sample	Radical polymerisation			Anionic polymerisation		
	Diameter (nm)	SD (nm)	PDI	Diameter (nm)	SD (nm)	PDI
1st step	162	47	0.127	337	138	0.514
2nd step	167	49	0.135	210	58	0.126
3rd step	158	40	0.099	680	263	0.398

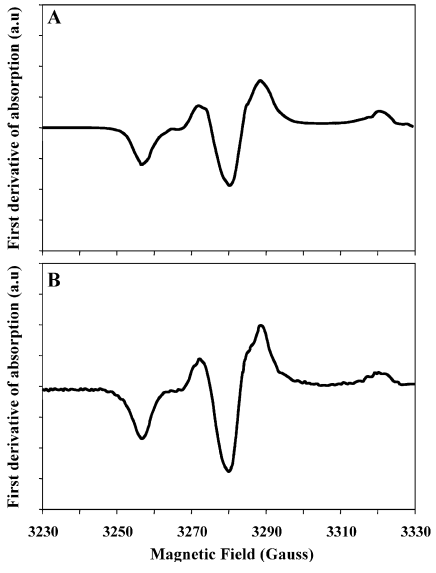

Fig. 3A, B Electronic paramagnetic resonance (EPR) spectra of freeze-dried particles obtained by two different polymerisation mechanisms. The intensity is given in arbitrary units (*a.u*). **A** Particles prepared by anionic polymerisation. **B** Particles prepared by radical polymerisation

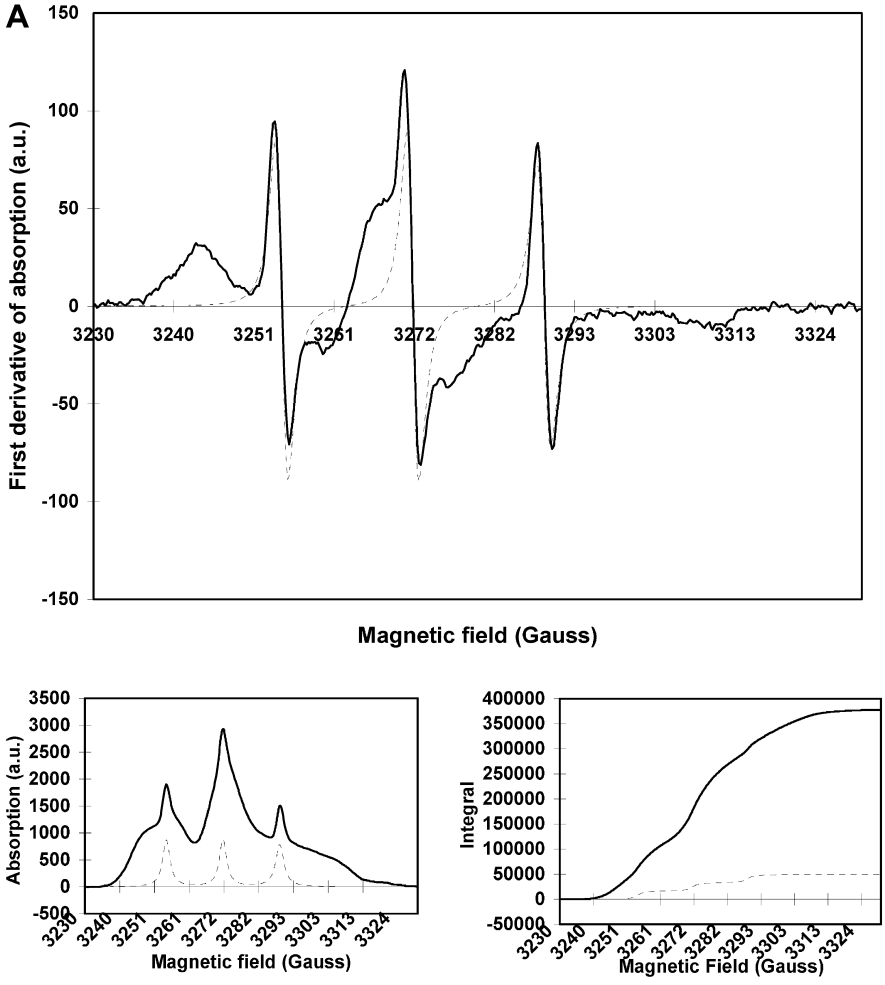

Fig. 4A, B EPR spectra of the rehydrated freeze-dried particles obtained by two different polymerisation mechanisms. **A** Particles prepared by anionic polymerisation. **B** Particles prepared by radical polymerisation. *Solid line* experimental data, *dotted thin line* simulation with the Kivelson theory

a curve with a pronounced shoulder for the particles prepared by radical polymerisation. The intensity of the signals obtained with the particles prepared by radical polymerisation was higher than that of the signals obtained with the particles prepared by anionic polymerisation. This difference may be due to the difference in size, and therefore in specific area, between the two types of nanoparticles. Concerning the rehydrated particles, spectra of both types of particles were very close and the shape was quite similar to the spectrum obtained for the dispersed particles prepared by radical polymerisation.

The spectra could be analysed according to the model of Kivelson in order to obtain information about the mobility of the label bound to dextran chains on the surface of the particles. The parameters characterising the mobility of the labelled dextran chains deduced from the correlation times are reported in Table 2. Considering rehydrated or dispersed nanoparticles, the mobility of the label at a molecular level appeared to be very similar (within experimental errors) whatever the method of preparation of the nanoparticle was, as shown by the value of the calculated correlation times. However, considering the movement of the dextran chains bearing the label, the percentage between the slow and the fast movements appeared to differ according to the mechanism of polymerisation used to prepare the nanoparticles. Indeed, a clear difference was highlighted comparing the rehydrated and the dispersed nanoparticles prepared by the anionic polymerisation. In contrast, these percentages were the same for both the rehydrated and the dispersed state of the nanoparticles prepared by radical polymerisation.

Isobutylcyanoacrylate (IBCA) has been polymerised in acidic aqueous dispersion according to two polymerisation mechanisms. In both cases, colloidal polymer particles were formed. In the absence of cerium (IV) ions, all the nucleophilic groups and anions present in the aqueous medium are theoretically able to initiate the polymerisation of IBCA and the polymerisation takes place according to an anionic mechanism [43]. In the very acidic conditions used in this study, the anionic polymerisation was rather slow [37]. As shown elsewhere, the initiation of the polymerisation was mainly induced by the hydroxyl groups of dextran, since at such

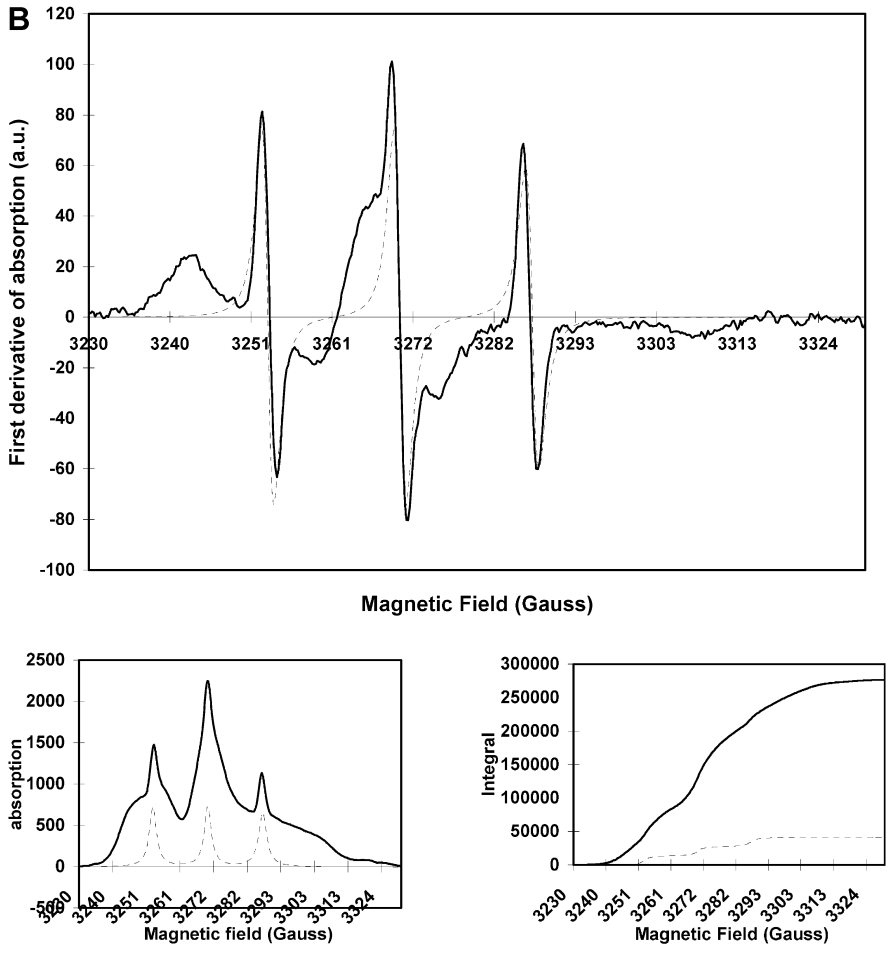

Fig. 4 (Contd).

a low pH the concentration of the hydroxyl ions resulting from water dissociation is too low and no polymerisation initiation could be initiated in pure water. The PIBCA chains growing on dextran lead to the formation of graft copolymers, with one dextran chain being able to bear several PIBCA chains (Fig. 6). In the presence of cerium (IV) ions, the initiation mechanism is different. Free radicals are created on the dextran chains after cleavage of a glycol function. In strongly acidic conditions such as those used in this study the sugar ring is then opened [44] and the polymerisation is actually initiated at the dextran chain end and followed by a fast propagation. This radical polymerisation occurred much faster than the anionic one [37] and the copolymer formed consisted of a linear diblock copolymer including dextran and PIBCA (Fig. 6).

In both cases, the copolymers consisting of an hydrophilic part including dextran and an hydrophobic part represented by PIBCA, were able to self-organise in such a way that the PIBCA would form the core of the colloidal particles and dextran would be exposed on the nanoparticle surface. Dextran chains present on the particle surface could be labelled with 4-amino-TEMPO containing a nitroxide free radical in order to investigate their mobility using EPR. Actually, the different polymerisation mechanisms used to produce these nanoparticles resulted in differences in the copolymer structure as explained above, and could therefore have led to a different arrangement of dextran chains on the particle surface. The coupling method used was specific to achieve the linkage of the label to dextran [40].

The dispersions obtained by radical polymerisation were very well defined and showed no aggregations and no changes in the course of the labelling process. This demonstrates a high stability, likely related to the presence of a repelling outermost brush structure. In contrast, particles obtained from the anionic polymerisation appeared less stable. Their size was twice that of the particles which resulted from radical polymerisation, and the suspensions contained aggregates. In addition, further aggregates appeared during the labelling and purification process. The poor stability of this nanodispersion may be due to a lower repelling capacity of the dextran shell surrounding the nanoparticle. In this polymerisation, one dextran chain is expected to bear several PIBCA chains, allowing them to form aggre-

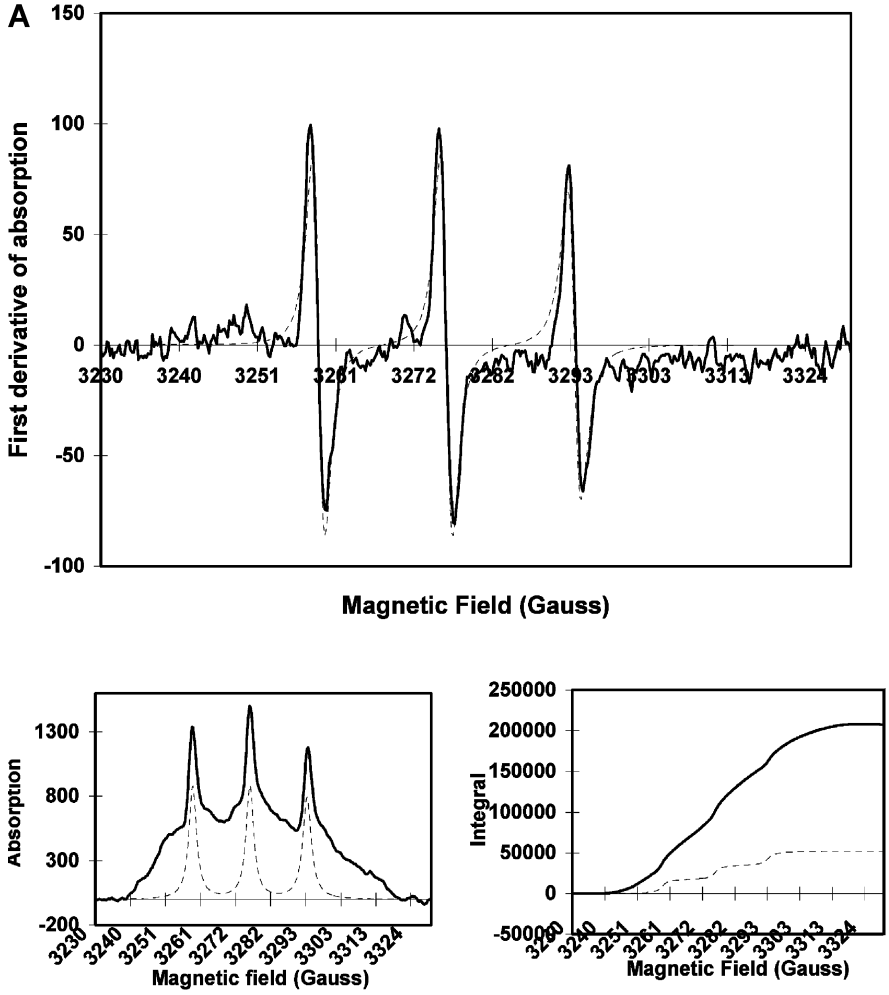

Fig. 5A, B EPR spectra of nanoparticles dispersed in water and obtained by two different polymerisation mechanisms. **A** Particles prepared by anionic polymerisation. **B** Particles prepared by radical polymerisation. *Solid line* experimental data, *dotted thin line* simulation with the Kivelson theory

gates. Thus, dextran chains should likely be attached to the core of the nanoparticle by several anchors resulting in the formation of loops and "trains" on the nanoparticle surface. In addition, some dextran chains of the graft copolymers could form bridges between two particles, resulting in formation of aggregates during anionic polymerisation.

EPR analysis of the rotational correlation time of the label grafted on dextran chain is related to its Brownian motion. It should give information about its movements when attached to dextran and therefore to the flexibility of the dextran chains located at the nanoparticle surface. The shapes of the different spectra obtained indicate that there were no interactions between bound labels and that the distance between labels was above 0.5 nm. Owing to the intensity of the signals observed in the EPR spectra, it should be highlighted that a sufficient amount of label was linked to the surface of both types of nanoparticles. This result confirmed that, during polymerisation, copolymers self-organised to give core-shell type particles in which dextran is located at the outside of the nanoparticles and is then accessible for further chemical modifications.

Very broad signals were shown by the EPR spectra given by freeze-dried particles indicating that the label moved slowly. In this state, dextran chains appeared immobile on the particle surface. In contrast, EPR spectra showing typical Lorentzian lines were obtained with rehydrated and dispersed particles. This indicated that a significant percentage of the label was mobile, and thus located on flexible parts of the dextran chains.

In the case of particles prepared by radical polymerisation, the spectra obtained with the rehydrated and dispersed samples were superimposed (see Fig. 4B and Fig. 5B), indicating that the mobility of the dextran chains was the same, regardless of the amount of the surrounding water. The rotational correlation times of the label, calculated from the spectra to evaluate the freedom of the label movement, were of the same order of magnitude ranging within experimental errors. It confirmed the same moving capacity of the dextran chains located on both the surface of rehydrated and

Fig. 5 (Contd).

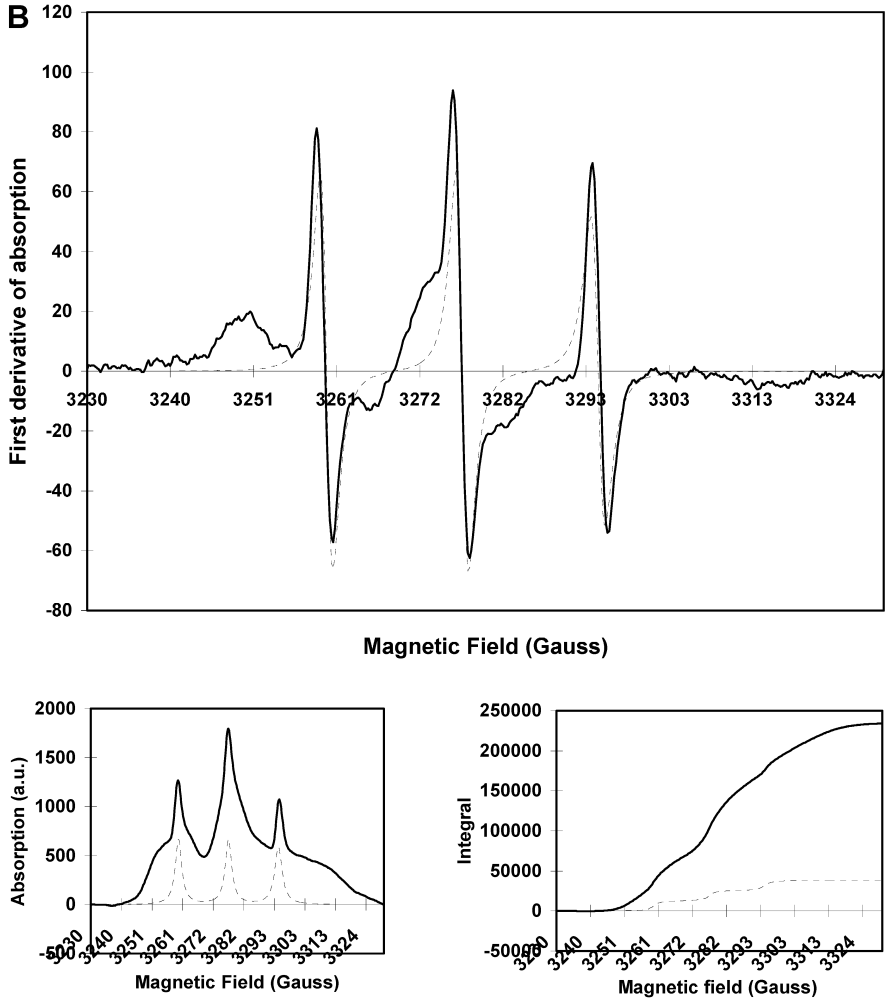

dispersed nanoparticles. With the rehydrated nanoparticles, the thickness of the hydrated layer should be rather small. Thus, this result suggests that dextran chains are very flexible and the particle surface was not significantly modified by the freeze-drying process. Indeed, a small amount of water was sufficient to totally recover the mobility of dextran chains after freeze-drying and rehydration. These results were also consistent with the presence of a repelling brush at the nanoparticle surface resulting from the binding of dextran chains by one end to the PIBCA core of the particles, and conferring a high stability to the dispersion.

However, considering the model of the arrangement of dextran chains as a brush at the nanoparticle surface, the ratio between fast- and slow-moving labels could appear surprising. This can be explained considering the position of the label along the dextran chains. Indeed, if the label is located close to the particle core, the length

Table 2 Summary of information calculated by using the Kivelson theory on spectra from Fig. 3, Fig. 4 and Fig. 5

Type of sample	Radical polymerisation			Anionic polymerisation		
	Slow movement (%)	Fast movement (%)	Correlation time (s)	Slow movement (%)	Fast movement (%)	Correlation time (s)
Freeze-dried particles	100 ± 2	0	–	100 ± 2	0	–
Rehydrated freeze-dried particles	85 ± 1.7	15 ± 0.3	1.2×10^{-10}	87 ± 1.8	13 ± 0.2	1.2×10^{-10}
Dispersed particles	84 ± 1.7	16 ± 0.3	1.6×10^{-10}	75 ± 1.5	25 ± 0.5	1.6×10^{-10}

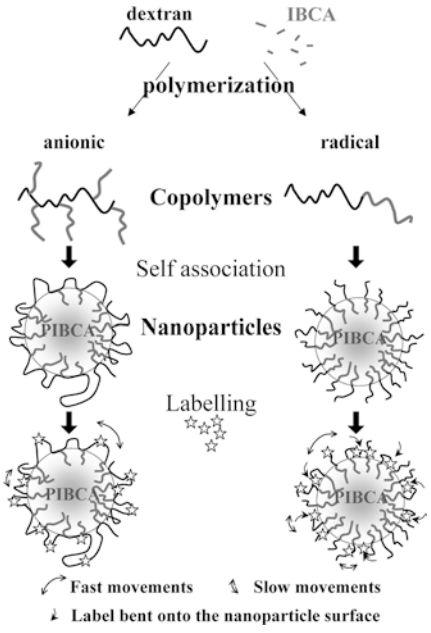

Fig. 6 Hypothesis about the conformation of the dextran chains at the nanoparticle surface depending on the mechanism of polymerisation of isobutylcyanoacrylate applied for the synthesis of the nanoparticles. The anionic polymerisation lead to the formation of a grafted copolymer with dextran backbone and poly(isobutylcyanoacrylate) (PIBCA) side chains which self organise in core-shell nanoparticles with dextran loops and trains at the surface of the PIBCA core. In the case of the radical polymerisation, a linear block copolymer including dextran and PIBCA self organise in nanoparticles with a brush of dextran chains at the surface of the PIBCA core

of the dextran chain between the anchor and the label will be too short to undergo large movements and to appear very mobile. On the contrary, if the label is far enough from the core, it can be very mobile, except if the chain is temporarily bent on the particle core because of the occurrence of hydrophobic interactions between the particle core and the label. In this case, the apparent mobility of the label evaluated experimentally would be reduced. In the concentration profile of segments starting from the surface, the thickness of the slow motion part could be higher than just one monomer unit. However, even if this phenomenon took place and because of the transient character of such a conformation, the stability of the particle suspension should not be affected.

The analysis of particles obtained by anionic polymerisation showed a decrease in the percentage of the fast movements after the particles have been freeze-dried and rehydrated. These results indicate that the freeze-drying process induced substantial modifications of the flexibility of the dextran chains. This is consistent with the rather low stability observed with these particles (Table 1). Label molecules endowed with fast movements could be attached quite far from the surface of the core of the nanoparticles, for instance on dextran chains forming large loops. It can be suggested that such loops would need more water than brushes to recover their mobility after freeze-drying. Slow movements of the label can be associated with labelling sites located close to the core of the nanoparticles, such as ''feet'' of large loops, smaller loops or ''trains'' corresponding to dextran chains collapsed onto the nanoparticle surface. This arrangement of the dextran chains on the surface of the particles is consistent with the graft structure of the copolymers formed during anionic polymerisation. Indeed, in this case one chain of dextran is anchored to the core of the nanoparticle by several PIBCA chains, as illustrated in Fig. 6. The ratio between slow and fast movements of the label coupled to these particles was also rather unexpected. However, the larger dextran loops are readily accessible for the coupling reaction to occur during labelling of the nanoparticles. In contrast, sites of reactions can be hindered in ''trains'' preventing the coupling reaction from occuring on dextran chains collapsed on the nanoparticle surface. Thus, the apparent mobility of the label as evaluated experimentally could mostly result from a rather high degree of labelling of the most accessible mobile loops. In the radical polymerisation the exchange between an extended and an adsorbed conformation can be rather frequent and portions of chains labelled at the outer periphery can rapidly become slow motion parts. In contrast, for the anionic polymerisation the distribution between loops and trains is much more fixed chemically, and portions of chains labelled at the outer periphery have a tendency to stay there without further treatment.

In conclusion, core-shell type nanoparticles were obtained by polymerisation of IBCA in emulsion performed in acidic medium according to two different polymerisation routes. In both cases, the polymerisations were initiated on dextran. The linear diblock copolymers resulting from the radical polymerisation self-organised into small and monodispersed well-stabilised nanoparticles. The graft copolymers resulting from anionic polymerisation self-organised into larger and less stable nanoparticles. Both types of particles were easily labelled with 4-amino-TEMPO and typical EPR spectra could be recorded, showing that dextran located at the nanoparticle surface could react with the spin label. The shapes of the spectra obtained for the two types of particles were different. Their analysis according to Kivelson theory revealed that a significant proportion of the label bound to dextran was mobile. In addition, this technique highlighted a difference in the mobilities of the dextran chains at the nanoparticle surface according to their method of preparation and degree of hydration (freeze-dried, rehydrated, or dispersed). The results of this study open up interesting possibilities of EPR for investigating the mobility of the chains of polysaccharides grafted on the surface of colloidal polymer parti-

cles. It could be interesting to study the effect of dextran chain length on their mobility at the nanoparticle surface, and to correlate EPR results with the capacity of the corresponding nanoparticles to adsorb proteins and to induce complement activation.

Acknowledgements The authors would like to thank Dr K. Broadley from Loctite for his kindness in providing isobutylcyanoacrylate, and Prof. P. Couvreur for his constant interest in this project and useful discussions. C. Chauvierre is a fellow of the Ministry of Research in France.

References

1. Barratt G, Couarraze G, Couvreur P, Dubernet C, Fattal E, Gref R, Labarre D, Legrand P, Ponchel G, Vauthier C (2001) Polymeric micro and nanoparticles as drug carriers.. In: Dumitriu S (ed) Polymeric biomaterials, 2nd edn. Dekker, New York, pp 753–782
2. Fattal E, Vauthier C (2002) Nanoparticles as drug delivery systems. In: Swarbrick J, Boylan JC (eds) Encyclopedia of pharmaceutical technology. Dekker, New York, pp 1874–1892
3. Couvreur P, Barrat G, Fattal E, Legrand P, Vauthier C (2002) Crit Rev Drug Del Systems 19:99
4. Kattan J, Droz JP, Couvreur P, Marino JP, Boutan-Laroze A, Rougier P, Brault P, Vranckx H, Grognet JM, Morge X, Sancho-Garnier H (1992) Invest New Drugs 10:191
5. Stella B, Arpicco S, Peracchia MT, Desmaële D, Hoebeke J, Renoir M, D'Angelo J, Cattel L, Couvreur P (2000) J Pharm Sci 89:1452
6. Li YP, Pei YY, Zhou ZH, Zhang XY, Gu ZH, Ding J, Zhou JJ, Gao XJ, Zhu JH (2001) Biol Pharm Bull 24:662
7. Li YP, Pei YY, Zhou ZH, Zhang XY, Gu ZH, Ding J, Zhou JJ, Gao XJ, Zhu JH (2001) J Control Release 71:287
8. Brigger I, Chaminade P, Marsaud V, Appel M, Besnard M, Gurny R, Renoir M, Couvreur P (2001) Int J Pharm 214:37
9. Calvo P, Gouritin B, Chacun H, Desmaële D, D'Angelo J, Noël JP, Georgin D, Fattal E, Andreux JP, Couvreur P (2001) Pharm Res 18:1157
10. Calvo P, Gouritin B, Brigger I, Lasmezas C, Deslys JP, Williams A, Andreux JP, Dormont D, Couvreur P (2001) J Neurosci Methods 11:151
11. Vauthier C, Couvreur P (in press) Miscellanous biopolymers and biodegradation of synthetic polymers. In: Matsumara JP, Steinbuchel A (eds) Handbook of biopolymers, vol 9. Wiley-VHC, New York
12. Brigger I, Dubernet C, Couvreur P (in press) Adv Drug Deliv Rev 54:631
13. Damgé C, Michel C, Aprahamiam M, Couvreur P (1988) Diabetes 37:246
14. Schwab G, Chavany C, Duroux I, Goubin G, Lebeau J, Helene C, Saison-Behmoaras T (1994) Proc Natl Acad Sci USA 91:10460
15. Desai SD, Blanchard J (2000) J Delivery Targeting Ther Agents 7:201
16. Fresta M, Fontana G, Bucolo C, Cavallaro G, Giammona G, Puglisi G (2001) J Pharm Sci 90:288
17. Fattal E, Youssef M, Couvreur P, Andremont A (1989) Antimicrob Agents Chemother 33:1540
18. Chianilkulchai N, Driouich Z, Benoit JP, Parodi AL, Couvreur P (1989) Sel Cancer Ther 5:1
19. Gibaut S, Andreux JP, Weingarten C, Renard M, Couvreur P (1994) Eur J Cancer 6:820
20. Gibaut S, Rousseau C, Weingarten C, Favier R, Douay L, Andreux JP, Couvreur P (1998) J Control Release 52:131
21. Jeon SI, Lee JH, Andrade JD, De Gennes PG (1991) J Coll Interface Sci 142:149
22. Gref R, Minamitake Y, Perrachia MT, Trubetskoy V, Torchilin V, Langer R (1994) Science 263:1600
23. Bazile D, Prud'homme C, Bassoullet MT, Marlard M, Spenlehauer G, Veillard M (1995) J Pharm Sci 84:493
24. Peracchia MT, Vauthier C, Puisieux F, Couvreur P (1997) Macromolecules 30:846
25. Mosqueira VCF, Legrand P, Gulik A, Bourdon O, Gref R, Labarre D, Barratt G (2001) Biomaterials 22:2967
26. Vittaz M, Bazile D, Spenlehauer G, Verrecchia T, Veillard M, Puisieux F, Labarre D (1996) Biomaterials 17:1575
27. Sahli H, Tapon-Bretaudière J, Fischer AM, Sternberg C, Spenlehauer G, Verrecchia T, Labarre D (1997) Biomaterials 18:281
28. Peracchia MT, Vauthier C, Puisieux F, Couvreur P (1997) J Biomed Mater Res 34:317
29. Gref R, Minamitake Y, Peracchia MT, Domb A, Trubetskoy V, Torchilin V, Langer R (1997) Pharm Biotechnol 10:167
30. Österberg E, Bergström K, Holmberg K, Schuman TP, Riggs JA, Burns NL, Van Alstine JM, Harris JM (1995) J Biomed Mater Res 29:741
31. Carreno MP, Maillet F, Labarre D, Jozefowicz M, Kazatchkine MD (1988) Biomaterials 9:514
32. Passirani C, Barrat G, Devissaguet JP, Labarre D (1998) Life Sci 62:775
33. Verdun C, Couvreur P, Vranckx H, Lenaerts V, Roland M (1986) J Control Release 3:205
34. Grislain L, Couvreur P, Lenaerts V, Roland M (1983) Int J Pharm 15:335
35. Olivier JC, Vauthier C, Taverna M, Puisieux F, Ferrier D, Couvreur P (1996) J Control Release 40:157
36. Chauvierre C, Couvreur P, Labarre D, Vauthier C (2002) Patent no. WO 02/39979
37. Chauvierre C, Labarre D, Couvreur P, Vauthier C (2003) Macromolecules 36:6018
38. Couvreur P, Kante B, Roland M, Guiot P, Bauduin P, Speiser P (1979) J Pharm Pharmacol 31:331
39. Hommel H (1995) Adv Colloid Interface Sci 54:209
40. Touhami A, Hommel H, Legrand AP, Serres A, Muller D, Jozefonvicz J (1993) Coll Surf B: Biointerfaces 1:189
41. Berliner LJ (1976) Spin labeling. Theory and applications. Academic, New York pp 592
42. Kivelson DJ (1960) J Chem Phys 33:1094
43. Eromosele IC, Pepper DC, Ryan B (1989) Makromol Chem 190:1613
44. Casinos I (1992) Polymer 33:1304